

Universality of spectra for interacting quantum chaotic systems

Wojciech Bruzda¹, Marek Smaczyński¹, Valerio Cappellini¹, Hans-Jürgen Sommers², and Karol Życzkowski^{1,3}

¹*Mark Kac Complex Systems Research Centre, Institute of Physics, Jagiellonian University, ul. Reymonta 4, 30-059 Kraków, Poland*

²*Fachbereich Physik, Universität Duisburg-Essen, Campus Duisburg, 47048 Duisburg, Germany*

³*Centrum Fizyki Teoretycznej, Polska Akademia Nauk, Al. Lotników 32/44, 02-668 Warszawa, Poland*

(Dated: Mar. 15, 2010)

We analyze a model quantum dynamical system subjected to periodic interaction with an environment, which can describe quantum measurements. Under the condition of strong classical chaos and strong decoherence due to large coupling with the measurement device, the spectra of the evolution operator exhibit an universal behavior. A generic spectrum consists of a single eigenvalue equal to unity, which corresponds to the invariant state of the system, while all other eigenvalues are contained in a disk in the complex plane. Its radius depends on the number of the Kraus measurement operators, and determines the speed with which an arbitrary initial state converges to the unique invariant state. These spectral properties are characteristic of an ensemble of random quantum maps, which in turn can be described by an ensemble of real random Ginibre matrices. This will be proven in the limit of large dimension.

I. INTRODUCTION

Time evolution of an isolated quantum system can be described by unitary operators. Quantum dynamics corresponds then to an evolution in the space of quantum pure states, since a given initial state $|\psi\rangle$ is mapped into another pure state $|\psi'\rangle = U|\psi\rangle$, where $U = \exp(-iH)$. Here H represents a Hermitian Hamiltonian of the system and the time t is set to unity.

If the underlying classical dynamics is chaotic the Hamiltonian H or the evolution operator U can be mimicked by ensembles of random unitary matrices [1, 2]. In particular, spectral properties of an evolution operator of a deterministic quantum chaotic system coincide with predictions obtained for the Dyson ensembles of random unitary matrices [3]. The symmetry properties of the system determine which ensemble of matrices is applicable. For instance, if the physical system in question does not possess any time-reversal symmetry, one uses random unitary matrices of the circular unitary ensemble (CUE). If such a symmetry exists and the dimension of the Hilbert space is odd one uses symmetric unitary matrices of the circular orthogonal ensemble (COE) [4].

If the quantum system S is not isolated, but it is coupled with an environment E , its time evolution is not unitary. One needs then to characterize the quantum state by a density operator ρ , which is Hermitian, $\rho = \rho^\dagger$, positive, $\rho \geq 0$ and normalized, $\text{Tr}\rho = 1$. Time evolution of such an open system can be described in terms of master equations [5], which imply that the dynamics takes place inside the set of quantum mixed states.

The coupling of the system S with an environment E can heuristically be described by adding to the Hamiltonian an anti-Hermitian component, $H \rightarrow H' = H - i\mu WW^\dagger$, where W is an operator representing the interaction between both systems [6]. The corresponding ensembles of non-Hermitian random matrices with spec-

trum supported on the lower half of the complex plane were studied in [7, 8]. For any positive value of the coupling strength parameter μ the dynamics of the system is not unitary and eigenvalues of the evolution operator move from the unit circle inside the unit disk – see Fig. 1b'. A similar situation occurs if one takes into account dissipation in the system. Such a dynamics of eigenvalues of a non-unitary evolution operator in the complex plane was analyzed by Grobe et al. [9] and later reviewed by Haake [1].

Time evolution of an open quantum system can also be described in terms of a global unitary dynamics V , which couples together a system S_A with an other subsystem S_B , followed by averaging over the degrees of freedom describing the auxiliary subsystem. Technically, the image of an initial state ρ of the system is obtained by a partial trace over the subsystem S_B , $\rho' = \text{Tr}_B[V(\rho \otimes \sigma)V^\dagger]$, where σ denotes the initial state of the environment. The map $\rho' = \Phi(\rho)$ defined in this way is completely positive and preserves the trace, so it is often called a *quantum operation* [10, 11]. Note that in this approach both *interacting* subsystems S_A and S_B are set on an equal footing. The second system, usually referred to as an 'environment', is in fact treated symmetrically, and one may also consider a dual operation, in which the partial trace is taken over the principal subsystem S_A – compare Fig. 1c.

A quantum map can be described by a *superoperator* Φ , which acts on the space of density operators. If N denotes the size of a density matrix ρ , the superoperator is represented by a matrix Φ of size N^2 . In general such a matrix is not unitary, but it obeys a quantum analogue of the Frobenius–Perron theorem, so its spectrum is confined to the unit disk [12]. Spectral properties of superoperators representing some exemplary interacting quantum systems were analyzed in [13–16]. It is worth to add that spectra of quantum superoperators are already experimentally accessible: Weinstein et al. [17] study spectra of superoperators corresponding to an NMR realiza-

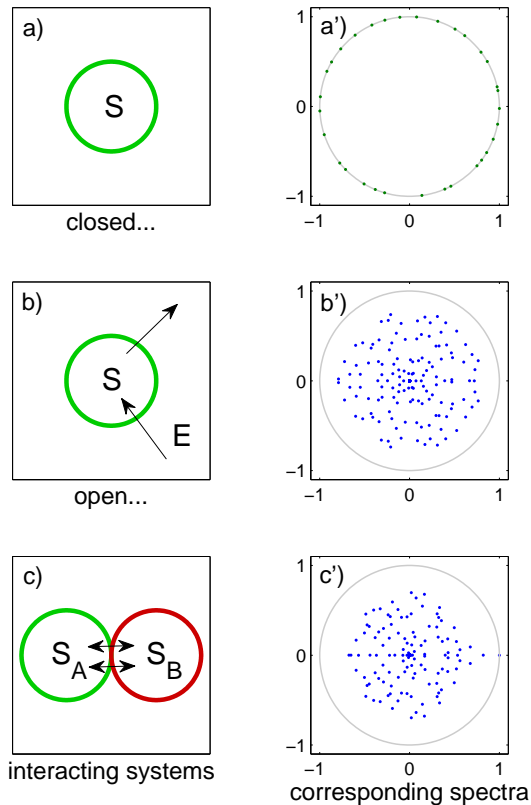


FIG. 1: Schematic representation of a) an isolated quantum system S characterized by a Hamiltonian H and a unitary evolution operator $U = \exp(-iH)$; b) open quantum system S . The influence of an environment E can be described by an anti-Hermitian part of the Hamiltonian, $-i\mu WW^\dagger$; and c) interacting systems S and E , in which the global evolution is unitary, and the non-unitarity of the evolution of S_A is due to the partial trace over the subsystem S_B . Panels a'), b') and c') show exemplary spectra of the corresponding evolution operators, which belong to the unit disk on the complex plane $z = x + iy$.

tion of exemplary quantum gates.

For a quantum operation Φ there exists an invariant state $\omega = \Phi(\omega)$. In a generic case of a typical (random) operation such an invariant state is unique [12]. If the action of the map is repeated n times any initial quantum state ρ converges to ω exponentially with the discrete time n . The rate of this convergence is governed by spectral properties of the superoperator, which can be characterized by the *spectral gap*, defined as the difference between moduli of the two largest eigenvalues.

The main aim of this work is to analyze spectra of evolution operators representing interacting quantum systems. We demonstrate that under the condition of strong classical chaos and strong decoherence these spectral properties are universal and correspond to an ensemble

of random operations [12]. In other words, we explore the link between quantum chaotic dynamics and ensembles of random matrices. The analysis performed earlier for unitary quantum dynamics [1] (see Fig. 1a) is extended for a more general case of non-unitary time evolution of interacting quantum systems. This problem can be described by an approach closely related to the one used earlier to characterize quantum dissipative dynamics. To describe spectra of such non-unitary evolution operators Grobe et al. [9] applied random matrices of the complex Ginibre ensemble [18].

The key idea of this work can be visualized in Fig. 2, which shows a bridge established between interacting quantum systems, appropriate ensembles of random operations and ensembles of Ginibre matrices. Since a superoperator describing one-step evolution operator can be represented as a real matrix [19], we are going to apply random matrices of *the real Ginibre ensemble* [20, 21]. In particular, we investigate time evolution of initially random pure states in a deterministic model of quantum baker map periodically subjected to quantum measurements, study the speed of their convergence to the invariant state and compare the results with those obtained for an appropriate ensemble of random operations.

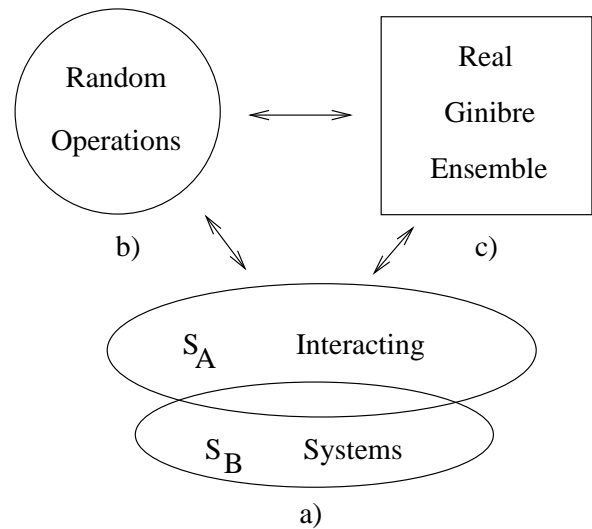


FIG. 2: Under the assumption of strong chaos and large decoherence a deterministic dynamics of a) an interacting quantum system can be described by b) an ensemble of random operations (completely positive, trace preserving maps). These, in turn, can be mimicked by c) random matrices of the real Ginibre ensemble, (which do not imply CP and TP properties).

This paper is organized as follows. In section II we recall necessary definitions and introduce several versions of a deterministic quantum system model: the quantum baker maps subjected to measurement process. In Section III we introduce various ensembles of random maps. In section IV the spectra and spectral gaps of superoperators corresponding to baker map are analyzed and com-

pared with the spectra of random operations. In section V we continue to analyze spectra of random quantum operations and give a proof for the real Ginibre conjecture put forward in [12], and we study the fraction of the real eigenvalues. For large dimension N this ratio is found in agreement with the predictions obtained for the real Ginibre ensemble.

II. QUANTUM OPERATIONS AND SPECTRAL GAP

We shall start reviewing the necessary notions and definitions. Let us define the set of quantum states \mathcal{M}_N which contains all Hermitian, positive operators ρ of size $N \times N$ with trace set to unity. A quantum linear map Φ acting on \mathcal{M}_N is called *completely positive* (CP) if positivity of the extended map, $(\Phi \otimes \mathbb{1}_M)(\rho) \geq 0 : \forall \rho$ holds for an arbitrary dimension M of the extension, and *trace preserving* (TP) if $\text{Tr}(\Phi(\rho)) = \text{Tr}(\rho)$. Any CP TP map is called quantum operation or *stochastic map*. If a quantum operation Φ preserves the identity, $\Phi(\mathbb{1}/N) = \mathbb{1}/N$, the map is called bistochastic.

According to the dilation theorem of Stinespring [22] any CP map may be represented by a finite sum of M Kraus operators,

$$\Phi(\rho) = \sum_{m=1}^M A^m \rho (A^m)^\dagger. \quad (1)$$

If the Kraus operators A^m satisfy the identity resolution, $\sum_m (A^m)^\dagger A^m = \mathbb{1}_N$, the map Φ is trace preserving. The corresponding superoperator can be expressed as a sum of the tensor products [10],

$$\Phi = \sum_{m=1}^M A^m \otimes (A^m)^*, \quad (2)$$

where the $*$ denotes the complex conjugation. Let z_i with $i = 1, \dots, N^2$ denote the spectrum of Φ ordered with respect to the moduli, $|z_1| \geq |z_2| \geq \dots \geq |z_{N^2}| \geq 0$.

A quantum stochastic map Φ sends the compact, convex set \mathcal{M}_N of mixed density matrices into itself. Hence such a map has a fixed point, the invariant quantum state $\omega = \Phi(\omega)$. Thus the spectrum of any superoperator Φ representing a quantum operation contains an eigenvalue z_1 equal to unity, while all other eigenvalues belong to the unit disk. In the case of unitary dynamics the leading eigenvalue is degenerated, but for a random stochastic map the invariant state is generically unique [12]. In this case any pure state, $|\psi\rangle\langle\psi|$, converges to the equilibrium state ω if transformed several times by the map Φ .

To analyze the rate of convergence to ω we analyze an average trace distance to the invariant states,

$$d(t) = \langle \text{Tr} |\Phi^t(\rho_0) - \omega| \rangle_\psi, \quad (3)$$

where t denotes the discrete time (i.e. the number of consecutive actions of the map Φ), while the average is

taken over the ensemble of initially random pure states, $\rho_0 = |\psi\rangle\langle\psi|$. In the case of a generic map an exponential convergence to equilibrium, $d(t) = d(0) \exp(-\alpha t)$ was reported [12]. The convergence rate depends on spectral properties of the superoperator Φ . The spectrum can be characterized by the *spectral gap*, $\gamma = 1 - |z_2|$, which generically determines the convergence rate, $\alpha = -\ln(1 - \gamma)$.

III. DETERMINISTIC SYSTEM: QUANTUM BAKER MAP SUBJECTED TO MEASUREMENTS

The formalism of discrete quantum maps is applicable to describe a deterministic quantum system, periodically interacting with an environment. In this work we concentrate on quantum dynamical systems, the classical analogues of which are known to be chaotic. Following the model of Balazs and Voros [23] we consider the unitary operator describing the one-step evolution model of quantum baker map,

$$B = F_N^\dagger \begin{bmatrix} F_{N/2} & 0 \\ 0 & F_{N/2} \end{bmatrix}. \quad (4)$$

Here F_N denotes the Fourier matrix of size N , $[F_N]_{jk} = \exp(ijk/2\pi N)/\sqrt{N}$ and it is assumed that the dimension N of the Hilbert space \mathcal{H}_N is even. The standard quantum baker map B may be generalized to represent an asymmetric classical map,

$$B_K = F_N^\dagger \begin{bmatrix} F_{N/K} & 0 \\ 0 & F_{N-N/K} \end{bmatrix} \quad (5)$$

where $K \geq 2$ is an integer asymmetry parameter chosen in such a way that the ratio N/K is integer. The standard model, obtained in the case $K = 2$, corresponds to the classically chaotic dynamics characterized by the dynamical entropy H equal to $\ln 2$ [24]. This system can be considered as a 2-dimensional lift of an 1-dimensional non-symmetric shift map,

$$f_K(x) = \begin{cases} Kx/(K-1) & : x \in [0, (K-1)/K] \\ Kx - K + 1 & : x \in ((K-1)/K, 1] \end{cases}. \quad (6)$$

Chaos in such a system can be characterized by its dynamical entropy, equal to the mean Lyapunov exponent, averaged with respect to the invariant measure of the classical system. Since the uniform measure is invariant with respect to the map f_K , the dynamical entropy h is equal to the mean logarithm of the slope df_K/dx ,

$$h(K) = \frac{1}{K} \ln K + \frac{K-1}{K} \ln \frac{K}{K-1}. \quad (7)$$

The entropy is maximal in the case $K = 2$, while in the limit $K \rightarrow \infty$ the entropy tends to zero. Hence the

larger value of the parameter K is, the weaker chaos in the classical system becomes.

In the case of the quantum system acting on the N -dimensional Hilbert space the largest possible value of the asymmetry parameter reads $K = N$. Thus the limiting case of the classically regular system cannot be obtained for any finite N . The limit of vanishing dynamical entropy, $h \rightarrow 0$, can be approached only in the classical limit $N \rightarrow \infty$ of the quantum system.

A generalized variant of a non-unitary baker map introduced by Saraceno and Vallejos described a dissipative quantum system [25]. In this work we study another model of non-invertible quantum baker map analyzed in [13, 26], which is deterministic, conserves the probability, and is capable to describe projective measurements or a coupling with an external subsystem.

In general there exist M different outcomes of the measurement process and thus the map is described by a collection of M Kraus operators. The simplest nontrivial case of $M = 2$ corresponds to dividing of the phase space into two parts, which we can choose to be the 'lower' and the 'upper' part. Such a measurement scheme allows one to write down the quantum operation corresponding to the 'sloppy baker map', in which both pieces of the classical phase space are not placed precisely one by another, but in each step an overlap of a positive width takes place. In the classical model the upper piece of the phase space is shifted down by $\Delta/2$ - see Fig. 3c - so the invariant measure lives in the rectangle of the width $(1 - \Delta)$.

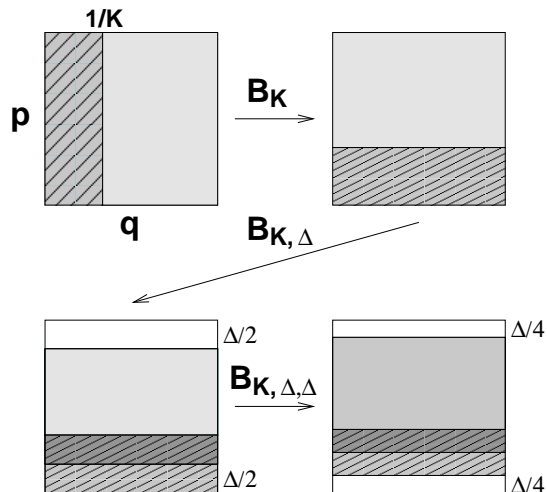


FIG. 3: Sketch of the classical dynamical system acting on the torus: b) reversible asymmetric ($K = 4$) baker map B_K , c) irreversible sloppy baker map $B_{K,\Delta}$ in which in each step the upper part of the phase space is shifted down by $\Delta/2$, d) double sloppy baker map $B_{K,\Delta,\Delta}$ in which both parts of the phase space are shifted vertically by $\Delta/4$.

To represent the shift in the quantum analogue of the map one uses a unitary translation operator V such that $V^N = \mathbb{1}_N$ and any momentum eigenstate $|k\rangle$ is shifted by one, $V|k\rangle = |k+1\rangle$. Hence the shift down by $\Delta/2$ is realized by the unitary operator, $V^{-N\Delta/2}$. Thus the

stochastic map describing the quantum sloppy map [13]

$$\Phi_{B_{K,\Delta}}(\rho) = D_b B_K \rho B_K^\dagger D_b^\dagger + D_t B_K \rho B_K^\dagger D_t^\dagger. \quad (8)$$

consists of two Kraus operators, which act on the unitarily rotated state $\rho' = B_K \rho B_K^\dagger$,

$$D_b = F_N^\dagger \begin{bmatrix} \mathbb{1}_{N/2} & 0 \\ 0 & 0 \end{bmatrix} F_N, \\ D_t = V^{-N\Delta/2} F_N^\dagger \begin{bmatrix} 0 & 0 \\ 0 & \mathbb{1}_{N/2} \end{bmatrix} F_N. \quad (9)$$

The operator D_b describes the projection on the lower part of the phase space, while the definition of the operator D_t includes also the operator representing the shift of the upper domain down by $\Delta/2$. Observe that the parameter Δ may take any real value from the unit interval $[0, 1]$. However, the case $\Delta = 0$ corresponds to the baker map without the shift but with a measurement, so it does not reduce to the standard unitary baker map B_K .

One can also consider another classical model of double sloppy map, in which both domains are simultaneously shifted by $\Delta/4$ towards the center of the phase space [27] - Fig. 3d. To write down the corresponding quantum model $B_{K,\Delta,\Delta}$ one needs thus to modify both Kraus operators, $D_b \rightarrow V^{N\Delta/4} D_b$ and $D_t \rightarrow V^{-N\Delta/4} D_t$.

Both variants of the model can be further generalized by allowing for a larger number M of measurement operators, represented by projectors on mutually orthogonal subspaces. For simplicity we assume here that the dimensionalities of all these subspaces are equal and read N/M . Varying the parameter M one may thus control the degree of the interaction of the baker system with the environment and study the relation between the decoherence in the interacting quantum system and the spectrum of the corresponding superoperator.

Increasing the asymmetry parameter K one can decrease the degree of classical chaos. To increase the degree of chaos one may just apply the quantum baker map twice, since the classical dynamical entropy of such a composite map is equal to $2 \ln 2$. In general one can allow for an arbitrary number of L of unitary evolutions, and replace unitary B by B^L . Alternatively one can say that the non-unitary measurement operation is performed only once every L periods of the unitary evolution. Choosing the parameter L to be of order of N one can assure that the quantum dynamics is as 'chaotic' as allowed by the quantum theory, what can be quantitatively characterized by the quantum dynamical entropy [28–30].

Therefore the generalized model of quantum sloppy baker map we are going to analyze here depends on the classical asymmetry parameter K , the width of the classical shift Δ , the number of free evolutions L , and the quantum parameter M denoting the number of measurement operators,

$$\Phi_{B_{\Delta,K,L,M}}(\rho) = \sum_{m=1}^M D_m (B_K)^L \rho (B_K^\dagger)^L D_m^\dagger. \quad (10)$$

Additionally, for each set of parameters of the model one can choose the appropriate set of projection operators D_m which correspond to the shift applied on one or on two parts of the classical phase space.

Note that the measurement process can also be interpreted as an interaction with a measurement apparatus, described by an auxiliary Hilbert space of M dimensions. Thus the model (10) represents an interacting quantum system and belongs to the general class of quantum operations defined by (1). A rich structure of the model and the possibility to tune independently several parameters of the quantum system allows us to treat this model as a valuable playground to investigate spectral properties of superoperators, which represent non-unitary dynamics of interacting quantum systems.

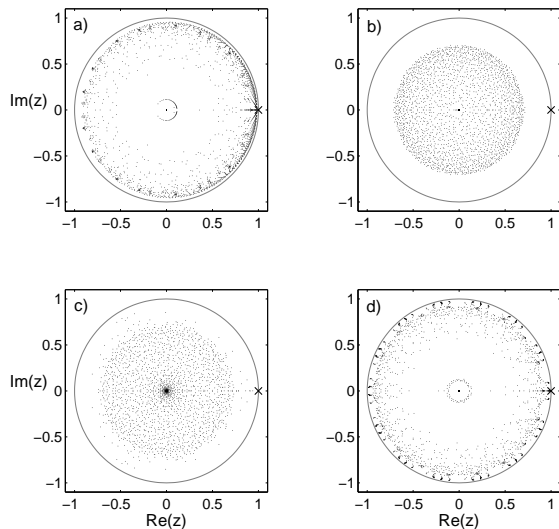


FIG. 4: Exemplary spectra of the evolution operator for the sloppy baker map for several values of the parameters of the model. The dimension of the Hilbert space $N = 64$, parameter $M = 2$, and the shift width $\Delta = 1/4$ are kept fixed. A generic spectrum for $K = 4, L = 16$ is shown on panel b). The subplots a) and c) are obtained for the cases of a weak classical chaos for $K = 64, L = 1$ and $K = L = 32$ respectively, while the last case d) shows the spectrum for the double sloppy map $B_{K,\Delta,\Delta}$ for $K = 64$ and $L = 64$.

We constructed quantum operations representing the generalized sloppy baker map (10) for several sets of the parameters of the model. In each case the superoperator Φ was obtained according to the expression (2) and diagonalized to yield the complex spectrum belonging to the unit disk.

In the case of several measurement operators, $M \geq 2$, the quantum baker map represents a non-unitary dynamics. Under the condition of classical chaos the leading eigenvalue $z_1 = 1$ is not degenerated and all remaining eigenvalues are located inside the disk of the radius equal to the modulus of the subleading eigenvalue $R = |z_2|$.

The spectra of the superoperator of the generalized sloppy baker map (10) were found to depend weakly on the shift parameter Δ . However, other parameters of the model (namely N, K, L and M) influence properties of the spectrum considerably - see Fig. 4.

As the asymmetry parameter K increases the difference between the sizes of two domains which form the classical phase space becomes larger. In the extreme limit of $K \rightarrow N \rightarrow \infty$ the classical system becomes only marginally chaotic, the eigenvalues are attracted to the unit circle and the spectral gap $\gamma = 1 - |z_2|$ disappears.

On the other hand, if we increase the degree of the classical chaos by increasing the number L of unperturbed unitary evolutions, the size of the spectral gap does not change, but the spectrum fills the complex disc of radius $R = |z_2|$ almost uniformly. Eventually, an increase of the number M of the measurements results in a faster decoherence in the system. This is reflected by an increase of the spectral gap γ . In fact the radius $R = 1 - \gamma$ of the disk supporting the spectrum decreases with M as $M^{-1/2}$. This observation - demonstrated in Fig. 7 - will be explained in section V.

IV. ENSEMBLES OF RANDOM OPERATIONS

In this section we propose three different ensembles of random stochastic maps acting on the space \mathcal{M}_N of mixed states of size N with different physical interpretation. We assume that all unitary matrices U used below are drawn according to the Haar measure on the unitary group of corresponding dimension unless stated otherwise.

1. *Environmental representation* of a random stochastic map [12]. Choose a random unitary matrix U of composite dimension NM and construct a random map as

$$\Phi_{\mathbb{E}}(\rho) = \text{Tr}_{\mathbb{E}} [U(\rho \otimes |\nu\rangle\langle\nu|)U^\dagger]. \quad (11)$$

It is assumed here that the environment, initially in an arbitrary pure state $|\nu\rangle$ is coupled with the system ρ by a random global unitary evolution U . The stochastic map is obtained by performing the partial trace over the M -dimensional environment.

2. *Random external fields* defined as a convex combination of M unitary evolutions [5]

$$\Phi_{\mathbb{R}}(\rho) = \sum_{m=1}^M p_m U_m \rho U_m^\dagger \quad (12)$$

where p_m are positive components of an arbitrary probabilistic vector of size M , $\sum_{m=1}^M p_m = 1$. All unitaries $U_m \in \mathbf{U}(N)$ are independent random Haar matrices. Random external fields form an example of bistochastic maps. They represent the physically relevant case in which the quantum system is subjected randomly with one of M given unitary operations and can also be interpreted as quantum iterated function systems [31].

3. *Projected Unitary Matrices* acting on states of a composite dimension, $N = KM$. All M Kraus operators are formed by unitarily rotated projection operators, $A_m = P_m U$ for $m = 1, \dots, M$ which leads to the map

$$\Phi_P(\rho) = \sum_{m=1}^M P_m U \rho U^\dagger P_m, \quad (13)$$

where U is a fixed random unitary matrix. Here $P_m = P_m^\dagger = P_m^2$ denote projective operators on K dimensional mutually orthogonal subspaces, which satisfy the identity resolution, $\bigoplus_m P_m = \mathbb{1}_N$. This ensemble of bistochastic maps corresponds to a model of deterministic quantum systems, in which unitary dynamics is followed by a projective measurement.

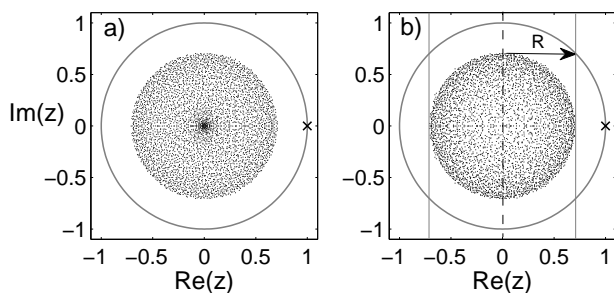


FIG. 5: Spectra of superoperators corresponding to typical random maps generated according to a) the ensemble Φ_E , and b) ensemble Φ_P (for definitions see Sec. II). All maps act on quantum states of size $N = 64$, while the parameter of the model reads $M = 2$. Note that in all cases the spectrum is contained in the disk of radius $R = 1/\sqrt{2}$ apart of the leading eigenvalue marked by 'x'.

In the ensembles of random maps defined above the integer number $M \geq 1$ determines the number of Kraus operators and serves as the only parameter of each ensemble of random maps. Observe that in the special case $M = 1$ the dynamics reduces to the unitary evolution, so both variants of the model are used to describe quantum systems with or without a generalized antiunitary symmetry [1].

As shown in [12] the flat measure in the set of stochastic matrices is obtained for the coupling of the system with an environment of dimension $M = N^2$, so that the Choi matrix, $D_\Phi := (\Phi \otimes \mathbb{1})|\phi_+\rangle\langle\phi_+|$ of size N^2 has full rank. Here $|\phi_+\rangle = \frac{1}{\sqrt{N}} \sum_{i=1}^N |i, i\rangle$ represents the maximally entangled state on the bipartite Hilbert space, $\mathcal{H}_N \otimes \mathcal{H}_N$. Due to the theorem of Choi the condition of complete positivity of the map is equivalent to positivity of the Choi matrix,

$$\Phi \text{ is CP} \Leftrightarrow D_\Phi \geq 0. \quad (14)$$

In general the discrete parameter M characterizes the strength of the non-unitary interaction and we shall vary

it from unity (unitary dynamics) to N^2 , which describes a generic random stochastic map.

We have generated several realizations of random maps from the ensembles Φ_E and Φ_P introduced above. Exemplary spectra of superoperators for maps pertaining ensembles obtained for $M = 2$ are shown in Fig. 5. In the latter case we superimposed the spectra from two realizations of the map Φ_P since by construction N^2/M eigenvalues of the superoperator are equal to zero.

In general, the spectra of random maps could be used to describe the spectra of deterministic system (10) under the condition of classical chaos and large decoherence.

Numerical results performed for various models of quantum maps reveal an exponential decay of the mean trace distance (3) to the invariant state. A comparison of such a time dependence of the mean trace distance d for quantum baker maps and random quantum maps is shown in Fig. 6. Interestingly, for a fixed system of size N the convergence rate α increases with the number of the measurements as $\alpha \sim \frac{1}{2} \ln M$, but it seems not to depend on the assumption, whether the global random evolution matrix U is taken from the orthogonal or unitary circular ensemble.

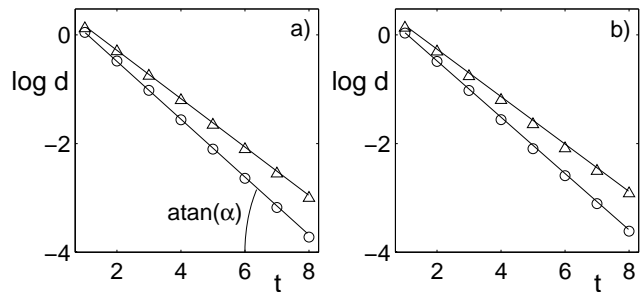


FIG. 6: Time dependence of the average trace distance d of random pure states to the invariant state for a) exemplary random quantum maps Φ_E and b) quantum baker map with parameters: $K = 4, L = 16, \Delta = 1/4$. Figure drawn in a log-scale shows the exponential decay for dimension $N = 24$ and parameters $M = 8$ (\circ) and $M = 12$ (\triangle). The average is taken over the set of 16 initial projectors.

Further numerical investigations confirm an expected relation between the size rate of the convergence of a typical quantum state towards the fixed point of the map and the spectral gap. As shown in Fig. 7 obtained for random operations as well as the generalized quantum baker map the radius $R = 1 - \gamma$ of the disk in the complex plane, which contains all but the leading eigenvalue, decreases with the number of measurements as

$$R = |z_2| \sim \frac{1}{\sqrt{M}}. \quad (15)$$

In the next section we present an explanation of this relation based on the theory of random matrices.

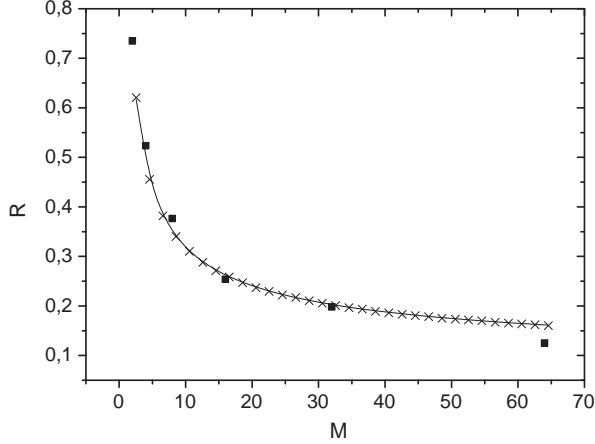


FIG. 7: Modulus of the subleading eigenvalue $R = |z_2|$ as a function of the dimension M of the environment for random quantum operation Φ_E for $N = 4$ (\times) and for the sloppy baker map for $N = 64, K = 4, L = 16, M = 2, \Delta = 1/4$ (\blacksquare). Solid line shows the fit according to eq. (15).

V. QUANTUM OPERATIONS AND REAL GINIBRE ENSEMBLE

Looking at the spectrum of a random stochastic map Φ_E shown in Fig. 5 one can divide the entire spectrum into three parts: i) a single eigenvalue $z_1 = 1$; ii) \mathcal{N}^{R} real eigenvalues distributed along the real line with a density $P^{\text{R}}(x)$, iii) remaining \mathcal{N}^{C} complex eigenvalues z_i , the distribution of which can be described by a density $P^{\text{C}}(z)$ on a complex plane.

Any density operator ρ of size N can be represented using the generalized Bloch vector representation

$$\rho = \sum_{i=0}^{N^2-1} a_i \lambda^i. \quad (16)$$

Here λ^i denotes the generators of $\text{SU}(N)$ such that $\text{Tr}(\lambda^i \lambda^j) = \delta^{ij}$ and $\lambda^0 \propto 1$. Since $\rho = \rho^\dagger$, $a_i \in \mathbb{R}$ for $i = 0, \dots, N^2-1$. The real vector $[a_0, \dots, a_{N^2-1}]$ is called the generalized Bloch vector. Thus

$$\Phi(\rho) = \sum_i \left(\sum_j \Phi^{ij} a_j \right) \lambda^i. \quad (17)$$

The Bloch vector can also be used to represent an arbitrary operation. Using Kraus operators A^m one represents the element Φ^{ij} of the superoperator Φ in a form

$$\Phi^{ij} = \text{Tr}(\lambda^i \Phi(\lambda^j)) = \text{Tr} \sum_m \lambda^i A^m \lambda^j (A^m)^\dagger, \quad (18)$$

where $i, j = 1, \dots, N^2 - 1$. This square matrix of order $N^2 - 1$ will be called \mathbf{C} . In a similar way we introduce

the vector κ and find that the remaining elements of the matrix Φ do vanish,

$$\Phi^{i0} = \text{Tr} \sum_m \lambda^i A^m \lambda^0 (A^m)^\dagger = \text{Tr} \lambda^i \lambda^0 \sum_m a_m (A^m)^\dagger \equiv (\kappa)_i \quad (19)$$

$$\Phi^{0j} = \text{Tr} \sum_m \lambda^0 A^m \lambda^j (A^m)^\dagger = \text{Tr} \lambda^0 \lambda^j = \delta^{0j}. \quad (20)$$

$$(21)$$

Hence the superoperator Φ can be represented as a real asymmetric matrix

$$\Phi_{ij} = \begin{bmatrix} 1 & 0 \\ \kappa & \mathbf{C} \end{bmatrix}, \quad (22)$$

where the $N' := N^2 - 1$ dimensional vector κ represents a translation vector while the $N' \times N'$ real matrix \mathbf{C} is a real contraction [12]. Thus the spectrum of Φ consists of the leading eigenvalue, equal to unity, and the spectrum of \mathbf{C} . Note that the complex eigenvalues of the real matrix \mathbf{C} appear in conjugated pairs, z and \bar{z} , which is a consequence of the fact, that the map Φ sends the set of Hermitian operators into itself, so as seen above the superoperator can be represented by a real matrix [19]. Since a map acting on states of size N is represented by a superoperator of dimension N^2 the following normalization relation holds, $1 + \mathcal{N}^{\text{R}} + \mathcal{N}^{\text{C}} = N^2$.

In the case that \mathbf{C} has only real eigenvalues one can bring \mathbf{C} by an orthogonal transformation \mathcal{O} to lower triangular form

$$\mathbf{C} = \mathcal{O}(\Xi + \Lambda)\mathcal{O}^{-1} \quad (23)$$

where $\Lambda = \text{diag}(z_1, \dots, z_{N'})$ while Ξ has elements only below the diagonal. Thus

$$d\mathbf{C} = \mathcal{O}[\mathcal{O}^{-1}d\mathcal{O}(\Xi + \Lambda) - (\Xi + \Lambda)\mathcal{O}^{-1}d\mathcal{O} + d\Xi + d\Lambda]\mathcal{O}^{-1}. \quad (24)$$

Hence the measure DC is given by

$$DC = \left| \prod_{i<j} (z_i - z_j) \prod_k dz_k \prod_{i<j} (\mathcal{O}^{-1}d\mathcal{O})_{ij} \prod_{j<i} d\Xi_{ij} \right| \quad (25)$$

where the Vandermonde determinant is the Jacobian of the transformation from $(\mathcal{O}^{-1}d\mathcal{O})_{ij}\Lambda_j$ to $(\mathcal{O}^{-1}d\mathcal{O})_{ij}$. Thus the measure $d\mu(\Lambda)$ has the form

$$D\mu(\lambda) = \left| \prod_{i<j} (z_i - z_j) \prod_k dz_k \right| \overline{\Theta(D_\Phi \geq 0)} \quad (26)$$

where in the last factor the positivity conditions of the corresponding Choi matrix is averaged by integrated over the measure $D\kappa D\Xi \prod \mathcal{O}^{-1}d\mathcal{O}$. This factor is expected to be a smooth function of the eigenvalues $z_1, \dots, z_{N'}$. In

the case that \mathbb{C} has a certain number of complex conjugate eigenvalues $D\mu(\Lambda)$ is of similar form, but the product of differentials dz_k has to be interpreted as exterior product [21]. It turns out that for large dimension N' the measure $d\mu(\Lambda)$ is given by the real Ginibre ensemble with the bulk of eigenvalues inside a certain disk in the complex plane. To prove this let us go back to the matrix representation of Φ in terms of M Kraus operators $A^m, m = 1, \dots, M$. Then

$$\Phi(\rho)_{ij} = \sum_{m=1}^M A_{ik}^m \rho_{kl} (A_{jl}^m)^* = \sum_{kl} \Phi_{ij,kl} \rho_{kl} \quad (27)$$

where A_{ik}^m are the matrix elements of Kraus operators and $*$ denotes the complex conjugation; $i, j, k, l = 1, \dots, N$. The Kraus operators obey

$$\sum_{m=1}^M \sum_{i=1}^N A_{ik}^m (A_{il}^m)^* = \delta_{kl} \quad (28)$$

thus it is natural to assume that A_{ik}^m represent N columns of a matrix U drawn from a circular unitary ensemble of dimension NM i.e. $U \in \mathbf{U}(NM)$. Using formulas by Mello [32] for the first four moments of $\mathbf{U}(NM)$ we are able to find exactly the first two moments of matrix elements $\Phi_{ij,kl}$. For example for $U \in \mathbf{U}(N) : \langle U_{b\beta} U_{a\alpha}^* \rangle = \delta_{ab} \delta_{\alpha\beta} / N$. Here $\langle \dots \rangle$ means the average over the unitary group. This implies here:

$$\langle \Phi_{ij,kl} \rangle = \sum_{m=1}^M \langle A_{ik}^m (A_{jl}^m)^* \rangle = \frac{1}{N} \delta_{ji} \delta_{lk}. \quad (29)$$

In this way we can derive the exact second moments:

$$\begin{aligned} \langle \Phi_{ij,kl} \Phi_{i\bar{j},k\bar{l}}^* \rangle &= \\ &= \frac{1}{(NM)^2 - 1} (M^2 \delta_{ij} \delta_{i\bar{j}} \delta_{kl} \delta_{k\bar{l}} + M \delta_{i\bar{i}} \delta_{j\bar{j}} \delta_{k\bar{k}} \delta_{l\bar{l}}) \\ &- \frac{1}{NM} \frac{1}{(NM)^2 - 1} (M^2 \delta_{ij} \delta_{i\bar{j}} \delta_{k\bar{k}} \delta_{l\bar{l}} + M \delta_{i\bar{i}} \delta_{j\bar{j}} \delta_{kl} \delta_{k\bar{l}}). \end{aligned} \quad (30)$$

We see that in the limit of large N the first two cumulants are identical to those of the Gaussian distribution (with variance $1/(N^2 M)$)

$$P(\Phi) \propto \exp \left(NM \sum_{ik} \Phi_{ii,kk} - \frac{N^2 M}{2} \sum_{ijkl} |\Phi_{ij,kl}|^2 \right). \quad (31)$$

The factor $1/2$ is due to the symmetry property $\Phi_{ij,kl} = \Phi_{ji,lk}^*$. We will argue below that for large M in addition the higher cumulants can be neglected. Hence the superoperator Φ associated with a random map can be described (up to the one eigenvalue 1) by the real Ginibre ensemble with eigenvalues inside a disk of radius $1/\sqrt{M}$, where M is the number of random Kraus operators defining Φ . This can also be seen by going back to the real matrix representation (18)-(22).

Let us now argue that for large M we can neglect higher cumulants. First of all for large N the elements A_{ik}^m , forming a minor of $U \in \mathbf{U}(NM)$, are essentially independent Gaussian variables with zero mean and variance $1/NM$. Thus as a consequence of the central limit theorem for large M $\Phi_{ij,kl}$ as sum of M essentially independent identically distributed variables is again Gaussian with variance $M/(NM)^2 = 1/N^2 M$. Also in the bulk the different matrix elements of Φ are independent. The average of $\Phi_{ij,kl}$ is given by $\delta_{ij} \delta_{kl} / N$.

To investigate the density of complex eigenvalues $z = x + iy$ of the superoperator Φ we analyzed their radial probability distribution $P(r)$, where $r = |z|$. The real eigenvalues are taken into account for this statistics. Fig. 8 shows a comparison of numerical data obtained for several realizations of quantum baker map, projective random operations and real random matrices pertaining to the Ginibre ensemble. The data are represented in the rescaled variable $r_M = r\sqrt{M}$ so that the radius of the disk of eigenvalues is set to unity. In all three cases displayed in the figure the radial density grows linearly, which corresponds to the flat distribution of eigenvalues inside the complex disk, in agreement with the predictions of the Ginibre ensemble. These results obtained for $N = 32$ show a smooth transition of the density in the vicinity of the boundary of the disk at $r_M = 1$, which becomes more abrupt for larger N . In the asymptotic case $N \rightarrow \infty$, the density of rescaled eigenvalues is described by the *circular law* of Girko,

$$P^{\mathbb{C}}(z) \sim \Theta(1 - |z|). \quad (32)$$

derived for complex Ginibre matrices.

The spectra of real random Ginibre matrices display a more subtle structure. A finite fraction of all eigenvalues are real, in analogy to the mean number of real roots of a real polynomial [33, 34]. Real eigenvalues of a real Ginibre matrix cover the real axis with a constant density. Furthermore, for large dimension the density of complex eigenvalues is known to be asymptotically constant in the complex disk except for a small region near the real axis [20].

To check for what random operations these effects can be observed in the spectrum of the superoperator we analyzed the average number $\langle \mathcal{N}^{\text{R}} \rangle_{\Phi}$ of real eigenvalues of the superoperator Φ . For any realization of Φ we have $\mathcal{N}^{\text{R}} = \#\text{REAL} / (N^2 - 1)$ where $\#\text{REAL}$ is the number of real eigenvalues of the real matrix of size $N' = N^2 - 1$. These data are compared with predictions for the real Ginibre ensemble, hereafter denoted by $\langle \mathcal{N}^{\text{R}} \rangle_{\text{RG}}$. The following expression for the mean number of real eigenvalues of a real Ginibre matrix of size $N^2 - 1$ was derived in [35-37]

$$\begin{aligned} \langle \mathcal{N}^{\text{R}} \rangle_{\text{RG}} &= 1 + \frac{\sqrt{2}}{\pi} \int_0^1 \frac{t^{1/2} (1 - t^{N^2 - 2}) dt}{(1 - t)^{3/2} (1 + t)} \\ &\simeq \sqrt{\frac{2}{\pi}} \sqrt{N^2 - 1} \quad \text{as } N \rightarrow \infty. \end{aligned} \quad (33)$$

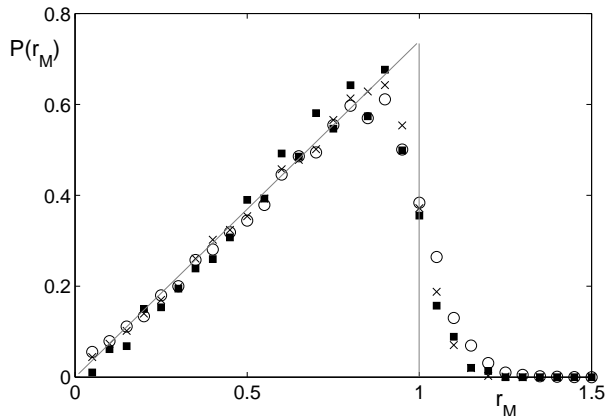


FIG. 8: Radial density of complex eigenvalues of spectra of superoperators corresponding to a deterministic model of sloppy baker map (\times), projective random operations (\circ) and the spectra of real random matrices of the Ginibre ensemble (\blacksquare). The size of each matrix is $N^2 = 32^2$, the number of Kraus operators is $M = 16$ so the density is shown as a function of the rescaled radius $r_M := r\sqrt{M} = 4r$. The tail of the distribution beyond the point $r_M = 1$ (equivalent to $r = 1/4$) does not violate therefore the quantum analogue of the Frobenius-Perron theorem.

These analytical results suggest to introduce a rescaled ratio

$$\eta := \frac{\langle \mathcal{N}^{\text{R}} \rangle_{\Phi}}{\sqrt{N^2 - 1}} \quad (34)$$

to make easier a comparison of data obtained for various systems of size N . Numerical results presented in Fig. 9 show that the superoperators associated with random maps are characterized by a non-zero fraction of real eigenvalues. In the case of strong interaction with the ancilla of the size $M = N^2$ the dynamical matrix D_{Φ} has full rank and the rescaled fraction of real eigenvalues of Φ coincides with the prediction for the real Ginibre ensemble.

To demonstrate further spectral features characteristic of the real Ginibre ensemble we analyzed spectra of superoperators and investigated the cross-section of the probability distribution $P(z)$ along the imaginary axis. Numerical data of this distribution denoted as $P_1^{\text{C}}(y)$ obtained for an ensemble of random maps Φ_{E} acting on the states of size $N = 3$ are shown in Fig. 10.

In order to compare these data with predictions of the real Ginibre ensemble we need to assure a suitable normalization. Let us rescale the imaginary axis as $y \mapsto y_M = \sqrt{M}y$, so that the rescaled formula (25) of [37] takes the form

$$\begin{aligned} P_1^{\text{C}}(y_M) &:= R_1^{\text{C}}(\sqrt{M}y) \\ &\simeq \sqrt{\frac{2M}{\pi}} \exp(2My^2) |y| \text{erfc}(|y|\sqrt{2M}). \end{aligned} \quad (35)$$

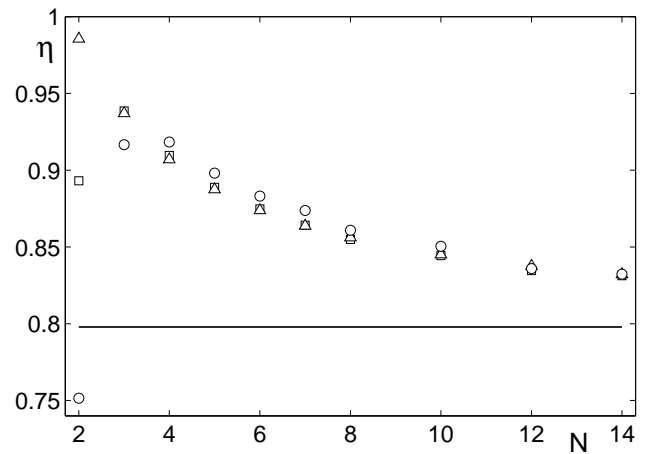


FIG. 9: Rescaled ratio of the real eigenvalues η of the superoperator for random operations with $M = N^2$ (\square), $M = N$ (\circ) and real Ginibre matrices (\triangle) as a function of the matrix size N . Solid horizontal line at $\sqrt{2/\pi}$ represents the asymptotic value of the normalized ratio implied by (33).

Making use of the standard estimations

$$\frac{1}{x + \sqrt{x^2 + 2}} < \exp(x^2) \int_x^{\infty} \exp(-t^2) dt \leq \frac{1}{x + \sqrt{x^2 + \frac{4}{\pi}}} \quad (36)$$

(see formula (7.1.13) at page 298 of Abramowitz and Stegun [38]), and the definition of the complementary error function $\text{erfc}(z)$, one obtains from eq. (35) an explicit form for lower and upper bounds for the rescaled distribution in the vicinity of the real axis

$$\frac{1}{\pi} \frac{2}{1 + \sqrt{1 + \frac{1}{My^2}}} \leq P_1^{\text{C}}(y_M) \leq \frac{1}{\pi} \frac{2}{1 + \sqrt{1 + \frac{2}{\pi My^2}}}. \quad (37)$$

As shown in Fig. 10 these bounds are rather precise and describe well the numerically observed density $P_1^{\text{C}}(y)$ of complex eigenvalues of the superoperators along the imaginary axis.

VI. CONCLUDING REMARKS

In this work we analyzed spectra of non-unitary evolution operators describing exemplary quantum chaotic systems and the time evolution of initially pure states. We have chosen to work with a generalized model of quantum baker map subjected to measurements [13, 27], which allows one to control the degree of classical chaos and the strength of the interaction with the environment. The size of the quantum effects, proportional to the ratio of the Planck constant to the typical action in the system, is controlled by the size N of the Hilbert space used to describe the quantum system. The classical limit of the quantum model corresponds to the limit $N \rightarrow \infty$.

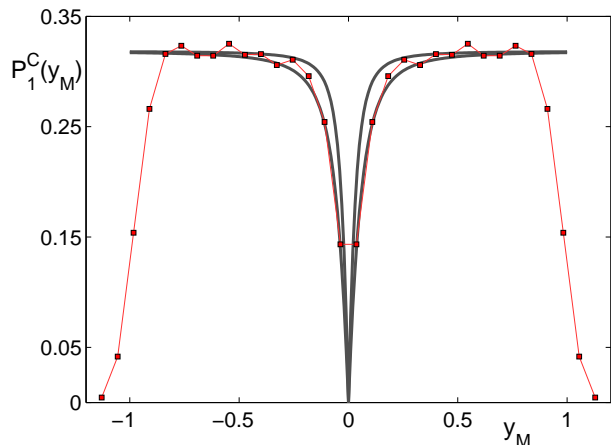


FIG. 10: Numerical data for the density $P_1^C(y_M)$ of complex eigenvalues along the rescaled imaginary axis obtained for an ensemble of random operations Φ_E of dimension $N = 8$ and with parameter $M = N^2 = 64$ (■) are compared with lower and upper bounds (37) obtained for small $|y|$ from the real Ginibre ensemble and represented by thick lines.

Due to a quantum analogue of the Frobenius–Perron theorem the evolution operator has at least one eigenvalue equal to unity, while all other eigenvalues are contained in the unit disk in the complex plane. In a generic case the leading eigenvalue is not degenerated and the corresponding eigenstate represents the unique quantum state invariant with respect to the evolution operator.

Investigating the time evolution of initially random pure states we found out that in a generic case they converge exponentially fast to the invariant state. The rate of this relaxation to the equilibrium depends on the size of the spectral gap, equal to the difference between the moduli of the first and the second eigenvalues of the evolution operator. In particular, the relaxation rate α was found to depend on the number of measurement operators M as $\frac{1}{2} \ln M$.

Spectral properties of evolution operators of deterministic quantum systems interacting with the environment

were compared with spectra of suitably defined ensembles of random matrices. Note that an idea to apply random matrices to model evolution operators of open deterministic quantum systems was put forward by Pełowski and Haake [39], but random maps used therein are not necessarily completely positive. This property is by construction fulfilled by the ensemble of random stochastic maps introduced in [12] and by two other ensembles of random bistochastic maps used in this work.

In general, the spectra of non-unitary operators corresponding to quantum deterministic systems display a wide variety of structures, which depend on classical parameters as the degree of chaos of the corresponding classical system characterized quantitatively e.g. by its dynamical entropy. The spectra depend also on quantum parameters as the dimension of the Hilbert space and the character of the interaction with the environment, which governs the strength of the decoherence effects. However, under an assumption of strong classical chaos and a uniform coupling of the system analyzed with all the states of the M -dimensional environment the spectral properties the corresponding evolution become *universal*: The spectrum consists of a leading eigenvalue equal to unity, while all other eigenvalues cover the complex disk of radius $R = 1/\sqrt{M}$.

In the asymptotic limit $N \rightarrow \infty$ the density of complex eigenvalues becomes uniform in the disk, besides the region close to the real axis. As the size of the environment M is equal to N^2 , which implies strong decoherence, the dynamical matrix D_Φ describing the quantum map Φ has full rank, so it can be considered as generic. In this very case the spectral statistics of this region of the complex spectrum of the superoperator and the fraction of its real eigenvalues coincides with predictions of the *real Ginibre ensemble*, a proof of which is given in this work.

Acknowledgements. It is a pleasure to thank R. Alicki for several fruitful discussions on various versions of the model of quantum interacting baker map.

Financial support by the Transregio-12 project der Deutschen Forschungsgemeinschaft and the special grant number DFG-SFB/38/2007 of Polish Ministry of Science and Higher Education is gratefully acknowledged.

-
- [1] F. Haake, *Quantum Signatures of Chaos*, II Ed. Springer, Berlin (2006).
 - [2] H.-J. Stöckman, *Quantum Chaos*, Cambridge Univ. Press (1999).
 - [3] F. J. Dyson, *J. Math. Phys.* **3**, No. 1, 140, 157, 166 (1962).
 - [4] M. L. Mehta, *Random Matrices*, III ed. Academic, New York (2004).
 - [5] R. Alicki, K. Lendi, *Quantum Dynamical Semigroups and Their Applications*, Springer, Berlin (1987).
 - [6] C. H. Lewenkopf, H. A. Weidenmüller, *Ann. of Phys.*, **212**, Issue 1, 53-83 (1991).
 - [7] F. Haake, F. Izrailev, N. Lehmann, D. Saher, H.-J. Sommers, *Z. Phys. B - Cond. Matter*, **88**, 359-370, (1992).
 - [8] Y. V. Fyodorov, H.-J. Sommers, *J. Phys. A: Math. Gen.* **36**, 3303 (2003).
 - [9] R. Grobe, F. Haake, H.-J. Sommers, *Phys. Rev. Lett.* **61**, 1899 (1986).
 - [10] M. A. Nielsen, I. L. Chuang, *Quantum Computation and Quantum Information*, Cambridge Univ. Press (2000).
 - [11] I. Bengtsson, K. Życzkowski, *Geometry of Quantum States*, Cambridge Univ. Press (2006).
 - [12] W. Bruzda, V. Cappellini, H.-J. Sommers, K. Życzkowski, *Phys. Lett A* **373**, 320-324 (2009).
 - [13] A. Łoziński, P. Pakoński, K. Życzkowski, *Phys. Rev. E* **66** 065210 (2002).

- [14] I. García-Mata, M. Saraceno, M. E. Spina, *Phys. Rev. Lett.* **91**, 064101 (2003).
- [15] I. García-Mata, M. Saraceno, *Modern Phys. Lett. B* **19**, 341, (2005).
- [16] J. M. Pedrosa, G. G. Carlo, D. A. Wisniacki, L. Ermann, *Phys. Rev. E* **79**, 016215 (2009).
- [17] Y. S. Weinstein, T. F. Havel, J. Emerson, N. Boulant, M. Saraceno, S. Lloyd, D. G. Cory, *J. Chem. Phys.* **121**, 6117 (2004).
- [18] J. Ginibre, *J. Math. Phys.* **6**, 440 (1965).
- [19] B. M. Terhal, D. DiVincenzo, *Phys. Rev.* **A61**, 22301 (2000).
- [20] N. Lehmann, H.-J. Sommers, *Phys. Rev. Lett.* **67**, 941 (1991).
- [21] H.-J. Sommers, W. Wicczorek, *J. Phys. A* **41** 405003 (2008).
- [22] W. F. Stinespring, *Proc. of the AMS*, 211-216 (1955).
- [23] N. L. Balazs, A. Voros, *Ann. Phys. (N. Y.)* **190**, 1 (1989).
- [24] E. Ott, *Chaos in dynamical systems*, II Ed. Cambridge University Press (2002).
- [25] M. Saraceno, R. O. Vallejos, *Chaos* **6**, 1054 (1996).
- [26] R. Alicki, A. Łoziński, P. Pakoński, K. Życzkowski, *J. Phys. A* **37** 5157 (2004).
- [27] M. Smaczyński, *Master thesis*, Jagiellonian University, Cracow 2009, see: <http://chaos.if.uj.edu.pl/~karol/prace/s09.pdf>.
- [28] W. Słomczyński, K. Życzkowski, *Phys. Rev. Lett.* **80**, 1880 (1998).
- [29] F. Benatti, V. Cappellini, M. De Cock, M. Fannes, D. Vanpeteghem, *Rev. Math. Phys.* **15**, 847-875 (2003).
- [30] V. Cappellini, *Acta Phys. Polon. A* **112**, 589-605 (2007).
- [31] A. Łoziński, K. Życzkowski, W. Słomczyński, *Phys. Rev. E* **68**, 046110 (2003).
- [32] P. A. Mello, *J. Phys. A: Math. Gen.* **23** 4061-4080 (1990).
- [33] E. Bogomolny, O. Bohigas, P. Leboeuf, *Phys. Rev. Lett.* **68**, 2726-2729 (1992).
- [34] G. Akemann, E. Kanzieper, *J. Stat. Phys.* **129**, 1159-1231 (2007).
- [35] A. Edelman, E. Kostlan, *Bull. Amer. Math. Soc.* **32**, 1-37 (1995).
- [36] A. Edelman, *Journal of Multivariate Analysis*, **60**, 203-232 (1997).
- [37] H.-J. Sommers, *J. Phys. A*, **40**, 671-676 (2007).
- [38] M. Abramowitz, I. A. Stegun, *Handbook of Mathematical Functions*, NBS, Washington, DC (1972).
- [39] P. Peplowski, F. Haake, *J. Phys. A* **26**, 2473 (1993).